REVIEW OF SCIENTIFIC INSTRUMENTS **87**, 036106 (2016)

Note: Enhancing the sensitivity of roll-angle measurement with a novel interferometric configuration based on waveplates and folding mirror

J. Qi,[1,a)] Z. Wang,[1] J. H. Huang,[1,a)] B. Yu,[1] J. Gao,[2] and S. Donati[3]
[1]*School of Mechanical Engineering, Xi'an Jiaotong University, Xi'an 710049, China*
[2]*State Key Laboratory for Manufacturing Systems Engineering, Xi'an Jiaotong University, Xi'an 710049, China*
[3]*Department of Industrial Engineering and Informatics, University of Pavia, Pavia 27100, Italy*

(Received 23 October 2015; accepted 23 February 2016; published online 8 March 2016)

A novel method for very high resolution measurement of roll angle on a transparent plate is developed theoretically and tested experimentally. The new optical configuration is based on the interferometric readout of phase shift accumulated on the double passage through half wave plate, together with a careful control of polarization state by means of quarter wave plate, and optimizing the tilt of the folding mirror. Sensitivity to roll angle is greatly enhanced and a gain coefficient exceeding 700 is found theoretically, based on Jones' matrix analysis, with a 6-fold increase respect to previous results. In the experimental setup, at the optimum 36° incidence to retroreflector, we measured a gain coefficient of 340. Correspondingly, with an interferometer phase meter resolving 0.01°, a roll-angle resolution 0.1-arc sec is attained. © *2016 AIP Publishing LLC.* [http://dx.doi.org/10.1063/1.4943297]

Measurement of geometric errors is an important task for accuracy compensation of Numerical Control (NC) machine tools. About angles, pitch and yaw angles are easily measured by conventional optical methods,[1,2] whereas roll angle, as an in-plane displacement, is more difficult to be obtained because it does not develop any optical phase shift to an external readout beam.

In this paper, we present an optical layout based on polarization-assisted conversion of the roll angle into an optical phase shift, read by a beam passing through the transparent plate actuated by the roll rotation. The phase shift is then read by a conventional two-frequency interferometer[3–8] resolving 0.01° by interpolation. Yet, this resolution is not enough to achieve a high resolution in roll angle measurement and calls for an enhancement of responsivity, or a gain coefficient G = ψ/α, where ψ is the optical phase shift and α is the roll angle. In numbers, we need the optical configuration be able to provide a gain G = 360 to attain roll angle resolution of 0.1-arc sec.

Previously, Liu[7] presented a system using a half wave plate (HWP) as the roll-sensing element, using a readout beam passing through HWP twice and a retroreflector right-angle prism. In a previous work,[9,10] we have demonstrated a variant based on multiple-pass through the HWP, so that a gain coefficient is developed (albeit at the expense of increased layout complexity).

In this paper, we present a novel optical configuration that makes available a much larger gain G compared to previous ones while retaining a simple optical structure.

The optical layout of the system is shown in Fig. 1. As the source, we use a commercial frequency stabilized He–Ne laser, based on the transversal Zeeman effect[9] and providing two orthogonal, linearly polarized modes with a frequency difference of about $f_1 - f_2$ = 730 kHz.

The output beam passes through a beam splitter (BS), and the reflected part is sent to a photodetector (PD_1) with a 45° oriented polarizer (P_1) so that the beating of the two modes generates the reference signal at the frequency difference $f_1 - f_2$.

The transmitted beam proceeds to a quarter wave plate (QWP) oriented at a small angle θ and becomes slightly elliptically polarized. This is the beam interrogating the roll-sensing element, a half wave plate (HWP), see Fig. 1. After passing through the HWP, the beam is folded back by a retroreflector (RM) made by two mirrors forming a right-angle dihedral and crosses the HWP again. Then, the beam is collected by the measurement photodetector (PD_2) preceded by a 45° polarizer (P_2). The electrical signal at the photodiode output has the same frequency $f_1 - f_2$ of the reference (PD_1) but is phase-shifted respect to reference of a quantity ψ = Gα carrying the roll-angle information.

The novelty of the configuration is that, by properly adjusting the incidence angle (o_1) at the first mirror surface of the retroreflector, a large gain coefficient is achieved, up to G = 720 theoretically and well in excess of 300 in the real experiment.

The Jones' calculus allows us to calculate amplitude and phase of the polarization mode components from input to output following the scheme of Fig. 1.

In the calculation, the beam propagation is along the z axis and x and y are set parallel to the two orthogonal linear polarized states (E_1 and E_2) of the input beam. The fast-axis of the QWP and the HWP is set as azimuth θ and α, respectively.

The Jones matrixes of the input beam and of the QWP, HWP, P, and the mirror are written as

$$E_0 = \begin{bmatrix} E_1 \\ E_2 \end{bmatrix} = \begin{bmatrix} A_1 \exp[i(\omega_1 t + \varphi_1)] \\ A_2 \exp[i(\omega_2 t + \varphi_2)] \end{bmatrix},$$

$$Q = \begin{bmatrix} \cos^2\theta + i\sin^2\theta & (1-i)\sin\theta\cos\theta \\ (1-i)\sin\theta\cos\theta & \sin^2\theta + i\cos^2\theta \end{bmatrix},$$

a)Authors to whom correspondence should be addressed. Electronic addresses: qijingya1991@126.com and huangjh@mail.xjtu.edu.cn.

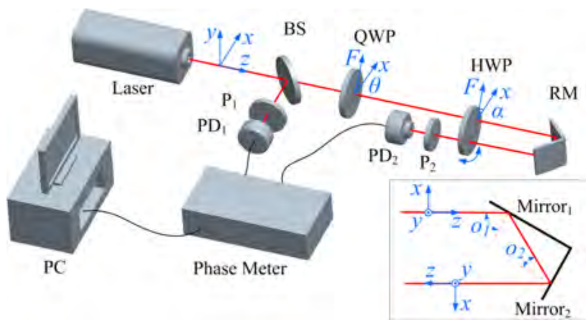

FIG. 1. Schematic configuration of the roll angle measurement system.

$$H(\alpha) = \begin{bmatrix} \cos 2\alpha & \sin 2\alpha \\ \sin 2\alpha & -\cos 2\alpha \end{bmatrix},$$
$$P = \begin{bmatrix} \cos 45^\circ & \sin 45^\circ \end{bmatrix},$$
$$M = \begin{bmatrix} r_p \exp(i\delta_p) & 0 \\ 0 & r_s \exp(i\delta_s) \end{bmatrix},$$

where r_p and r_s are the reflection amplitude ratio of the p-component and s-component, respectively, and δ_p and δ_s are the phase change upon reflection of p-component and s-component.[9] The relationship between r_s, δ_s, r_p, δ_p, and incident angle (o) has been computed following Ref. 10 and the results are shown in Fig. 2.

Then, the Jones matrixes of Mirror$_1$ and Mirror$_2$ are given as

$$M_1 = \begin{bmatrix} r_{1p} \exp(i\delta_{1p}) & 0 \\ 0 & r_{1s} \exp(i\delta_{1s}) \end{bmatrix},$$
$$M_2 = \begin{bmatrix} r_{2p} \exp(i\delta_{2p}) & 0 \\ 0 & r_{2s} \exp(i\delta_{2s}) \end{bmatrix},$$

where r_{1p}, r_{1s}, δ_{1p}, δ_{1s} in M_1 and r_{2p}, r_{2s}, δ_{2p}, δ_{2s} in M_2 are obtained by the incident angle of mirrors (o_1 and o_2) from Fig. 2.

The matrix of the measurement beam is written as

$$E_m = PH(-\alpha)M_2M_1H(\alpha)QE_0. \qquad (1)$$

Substituting the above values into Eq. (1), we get the AC measurement signal as

$$I_m(\sim) = k_m \cos[(\omega_1 - \omega_2)t + (\varphi_1 - \varphi_2) + \psi]. \qquad (2)$$

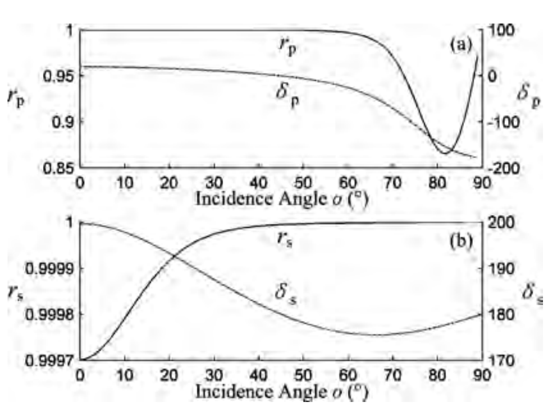

FIG. 2. Relationship between r_p, δ_p, r_s, δ_s and incidence angle of mirror o.

The AC reference signal is just the first two terms in Eq. (2), and subtracting it from the measurement phase, we get the phase shift ψ as

$$\psi = \tan^{-1}(p_1/q_1) - \tan^{-1}(p_2/q_2), \qquad (3)$$

where

$$\begin{aligned} p_2^1 = {} & r_{1p}r_{2p}\cos(2\alpha+\frac{\pi}{4})[\genfrac{}{}{0pt}{}{\cos\theta}{\sin\theta}\cos(2\alpha-\theta)\sin(\delta_{1p}+\delta_{2p}) \\ & \genfrac{}{}{0pt}{}{-\sin\theta}{+\cos\theta}\sin(2\alpha-\theta)\cos(\delta_{1p}+\delta_{2p})] \\ & +r_{1s}r_{2s}\sin(2\alpha+\frac{\pi}{4})[-\genfrac{}{}{0pt}{}{\cos\theta}{\sin\theta}\sin(2\alpha-\theta)\sin(\delta_{1p}+\delta_{2p}) \\ & \genfrac{}{}{0pt}{}{-\sin\theta}{+\cos\theta}\cos(2\alpha-\theta)\cos(\delta_{1p}+\delta_{2p})], \\ q_2^1 = {} & r_{1p}r_{2p}\cos(2\alpha+\frac{\pi}{4})[\genfrac{}{}{0pt}{}{\cos\theta}{\sin\theta}\cos(2\alpha-\theta)\cos(\delta_{1p}+\delta_{2p}) \\ & \genfrac{}{}{0pt}{}{+\sin\theta}{-\cos\theta}\sin(2\alpha-\theta)\sin(\delta_{1p}+\delta_{2p})] \\ & +r_{1s}r_{2s}\sin(2\alpha+\frac{\pi}{4})[-\genfrac{}{}{0pt}{}{\cos\theta}{\sin\theta}\sin(2\alpha-\theta)\cos(\delta_{1p}+\delta_{2p}) \\ & \genfrac{}{}{0pt}{}{+\sin\theta}{-\cos\theta}\cos(2\alpha-\theta)\sin(\delta_{1p}+\delta_{2p})]. \end{aligned}$$

The light intensity is given by

$$k_m = 2A_1A_2\sqrt{(p_1{}^2+q_1{}^2)(p_2{}^2+q_2{}^2)}. \qquad (4)$$

In Fig. 3, we plot the calculated phase shift ψ versus roll angle α for two values of the folding mirror incidence angle o_1 (45° and 36°), for $\theta = 2°$ (optimized ellipticity). The absolute value of maximal slope (AMS) of the curve is the gain coefficient G. Note that the AMS for $o_1 = 36°$ (point B in Fig. 3(b)) is much higher than the AMS for $o_1 = 45°$ (point A in Fig. 3(a)), the normal incidence angle of a folding mirror device.

So, our system achieves a higher gain coefficient in the optimal point, set o_1 around 36°. The slope of the local region is given by the differential of Eq. (3) as

$$K_\alpha = d\psi/d\alpha = m_1/n_1 - m_2/n_2, \qquad (5)$$

where

$$\begin{aligned} m_2^1 = {} & r[{}^{+}_{-}\cos 2\theta \sin(4\alpha - 2\theta)\sin\delta {}^{-}_{+} \sin 2\theta \cos\delta] \\ & + r\sin(4\alpha + \frac{\pi}{2})\sin\delta \\ & {}^{-}_{+}\sin 2\theta[r^2\cos^2(2\alpha + \frac{\pi}{4}) + \sin^2(2\alpha + \frac{\pi}{4})], \end{aligned}$$

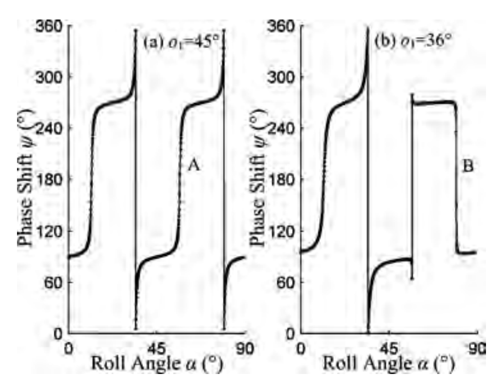

FIG. 3. Calculated phase shift ψ versus roll angle α for incidence at $o_1 = 45°$ and $o_1 = 36°$.

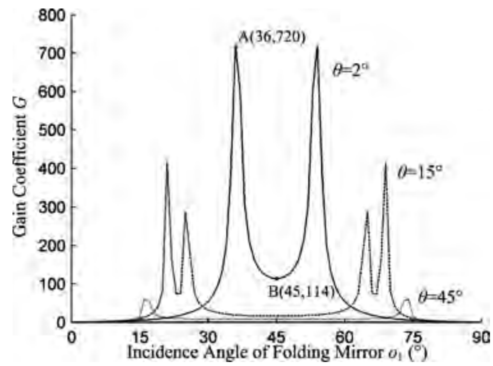

FIG. 4. Calculated gain coefficient versus incidence angle o_1 with ellipticity θ as a parameter.

$$n_2^1 = r^2\cos^2 2\alpha\left[{}^{\cos^2\theta}_{\sin^2\theta}\cos^2(2\alpha-\theta) + {}^{\sin^2\theta}_{\cos^2\theta}\sin^2(2\alpha-\theta)\right]$$
$$+\sin^2 2\alpha\left[{}^{\cos^2\theta}_{\sin^2\theta}\sin^2(2\alpha-\theta) + {}^{\sin^2\theta}_{\cos^2\theta}\cos^2(2\alpha-\theta)\right]$$
$$+\frac{r}{2}\sin 4\alpha\left[{}^{-}_{+}\cos 2\theta\sin(4\alpha-2\theta)\cos\delta{}^{-}_{+}\sin 2\theta\sin\delta\right],$$
$$r = \left(r_{1p}\cdot r_{2p}\right)/\left(r_{1s}\cdot r_{2s}\right), \quad \delta = \left(\delta_{1p}+\delta_{2p}\right)-\left(\delta_{1s}+\delta_{2s}\right).$$

From Eq. (5), we find that the gain coefficient curve is symmetrical with respect to the incidence angle $o_1 = 45°$, as shown in Fig. 4. At increasing input beam ellipticity θ, the folding mirror needs more tilt to get the highest gain coefficient.

The gain coefficient is up to 720 with $o_1 = 36°$ (or 54°) for $\theta = 2°$ (point A in Fig. 4), with a 6-fold improvement respect to the normal mirror set at $o_1 = 45°$ (point B in Fig. 4), used in previous papers.

The experimental setup is built according to Fig. 1. The laser emits two modes orthogonally polarized, with a frequency offset of 730 kHz. The folding mirror is fixed onto a precision rotary table with resolution of 0.1° and the incidence angle o_1 can be adjusted by the rotary table along the x axis. The HWP is mounted in a precision plate frame with rotary resolution of 1.7 min of arc. In the experiment, we set $\theta = 2°$ and measured the phase shift ψ by a CH6000A phase meter. To get high gain coefficient, we adjusted o_1 near 36° and rotate the HWP every 2°. The experimental result of ψ versus roll angle α agrees with the theoretical one as shown in Fig. 5 in which the AMS is located between points A and B. Rotate the HWP until the AMS is reached for three times. The experimental results of ψ versus roll angle α are shown in Fig. 6(a). The gain coefficient attained G = 340 and the response is fairly linear over a range of 0.3° of roll angle with fitting correlation coefficient higher than 0.99. Ideal resolution of the measurement is about 0.1-arc sec with the phase meter resolving 0.01°. The phase shift residuals δ_ψ between the average of experimental data and the fit shown in Fig. 6(b) are mainly caused by two reasons as follows: First, the rotary accuracy of HWP results that the roll angle α in Fig. 6(a) is not strictly 1.7-min of arc for every step. It can be eliminated with a high precision frame. Second, the signal fluctuation of the phase meter shown in Fig. 6(c) brings reading error for the phase shift, which can be reduced by using photo detector and laser with high performance.

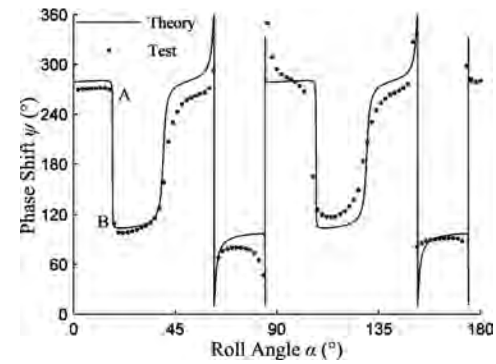

FIG. 5. Experimental result for $o_1 = 36°$ in the range of 180°.

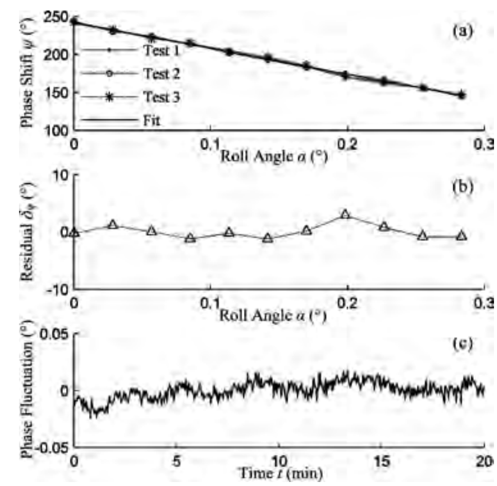

FIG. 6. Experimental result for $o_1 = 36°$.

The proposed configuration has demonstrated a large gain G = 340 and approaches the target of 0.1-arc sec resolution in the measurement of roll angle. The interferometer setup is sturdy and provides environmental noise immunity due to the common path and heterodyne design. So, it appears suitable for applications in the mechanical workshop environment.

This work is supported by the National Nature Science Foundation of China under Grant No. 61405156.

[1]S. Donati, *Electro-Optical Instrumentation: Sensing and Measuring with Laser* (Prentice Hall, New York, 2004), p. 125.
[2]M. Ikram and G. Hussain, Appl. Opt. **38**, 113 (1999).
[3]B. P. Coronkevich, G. G. Tarasov, and B. A. Hanov, Automeasurement **1**, 68 (1974) (in Russian).
[4]H. Jiang and C. Yin, Opt. Eng. **39**, 516 (2000).
[5]C. M. Wu and Y. T. Chuang, Sens. Actuators, A **116**, 145 (2004).
[6]L. Zhong, Z. Wang, S. Tang, J. Gao, and J. Guo, J. Xi'an Jiaotong Univ. **47**, 99 (2013) (in Chinese).
[7]Z. Liu and D. Lin, Sens. Actuators, A **104**, 127 (2003).
[8]S. Tang, Z. Wang, and M. Li, Rev. Sci. Instrum. **86**, 096104 (2015).
[9]Z. Li, Z. Wang, J. Huang, S. Tang, and J. Guo, J. Xi'an Jiaotong Univ. **48**, 112 (2014) (in Chinese).
[10]Z. Li, Z. Wang, J. Huang, J. Qi, B. Yu, and J. Guo, Chin. J. Lasers **42**, 0316002 (2015) (in Chinese).